Nanoscale Res Lett (2010) 5:1817–1821
DOI 10.1007/s11671-010-9718-7

NANO EXPRESS

Low-Temperature Preparation of Superparamagnetic $CoFe_2O_4$ Microspheres with High Saturation Magnetization

Hong Lei Yuan · Yong Qiang Wang · Shao Min Zhou · Li Sheng Liu · Xi Liang Chen · Shi Yun Lou · Rui Jian Yuan · Yao Ming Hao · Ning Li

Received: 23 May 2010 / Accepted: 26 July 2010 / Published online: 11 August 2010

Abstract Based on a low-temperature route, monodispersed $CoFe_2O_4$ microspheres (MSs) were fabricated through aggregation of primary nanoparticles. The microstructural and magnetic characteristics of the as-prepared MSs were characterized by X-ray diffraction/photoelectron spectroscopy, scanning/transmitting electron microscopy, and vibrating sample magnetometer. The results indicate that the diameters of $CoFe_2O_4$ MSs with narrow size distribution can be tuned from over 200 to ~330 nm. Magnetic measurements reveal these MSs exhibit superparamagnetic behavior at room temperature with high saturation magnetization. Furthermore, the mechanism of formation of the monodispersed $CoFe_2O_4$ MSs was discussed on the basis of time-dependent experiments, in which hydrophilic PVP plays a crucial role.

Keywords Magnetism · Nanostructure · Superparamagnetism

Introduction

Over the past decades, superparamagnetic (SP) nanostructures of spinel ferrites (MFe_2O_4: M = Fe, Co, Cu, Zn, etc.) have drawn intense scientific and technological interests because they possess a wide range of applications in magnetic fluid [1–3], magnetic resonance imaging (MRI) [4, 5], and drug delivery technology [6–8]. Recently, spinel cobalt ferrite ($CoFe_2O_4$) nanostructure materials have been extensively studied because they form a magnetic system which is an ideal candidate toward understanding and controlling magnetic properties at the atomic level through chemical manipulation [9]. Based on different techniques, SP $CoFe_2O_4$ nano-scale particles have been synthesized by several research groups [10–13]. Unfortunately, these small nanoparticles, especially those with sizes below 10 nm, have poor magnetic response abilities [14]. The low magnetization properties caused by small size limit their usage in a number of practical applications since they cannot be effectively manipulated by using moderate magnetic fields [15, 16]. In order to obtain a high saturation magnetization (Ms), simply making particles larger cannot be an option at all, resulting in a strong aggregation due to the non-SP ferromagnetic attraction [17].

Recently, much effort has been focused on the preparation of large-size SP particles with high Ms using simple composites [18, 19]. For example, Lee et al. [18] reported the fabrication of highly uniform SP mesoporous spheres with sub-micrometer scale, composed of silica and $CoFe_2O_4$ achieved a high magnetization value. Similar efforts were done by Bao et al. [19] in which controlled growth of SP nanostructures of spherical and rod-like $CoFe_2O_4$ nanocrystals. However, their high Ms required a high reaction temperature and expensive high-boiling point toxic solvents, which are disadvantages for their biological applicability. Moreover, such composite nanostructures are incompatible with low expense of preparing procedure. Herein, we report a single-step process for high-performance monodisperse SP $CoFe_2O_4$ MSs at low temperature (at only 180°C). As a consequence of the low-temperature synthesis, the as-obtained samples possess a high Ms (over 55 emu/g) and biocompatibility.

H. L. Yuan · Y. Q. Wang · S. M. Zhou (✉) · L. S. Liu · X. L. Chen · S. Y. Lou · R. J. Yuan · Y. M. Hao · N. Li
Key Lab for Special Functional Materials of Ministry of Education, Henan University, 475004 Kaifeng, People's Republic of China
e-mail: smzhou@henu.edu.cn

Experimental Section

Cobalt acetate [$Co(CH_3COO)_2 \cdot 4H_2O$], anhydrous ethanol ($CH_3CH_2OH$), iron(III) nitrate nonahydrate [$Fe(NO_3)_3 \cdot 9H_2O$], and poly(vinyl pyrrolidone) (PVP, K30) are of analytic grade reagents and purchased without further treatment. In a typical reaction, 2 mmol $Co(CH_3COO)_2 \cdot 4H_2O$ and 4 mmol $Fe(NO_3)_3 \cdot 9H_2O$ were dissolved in 35 mL CH_3CH_2OH forming a reddish brown solution, after which 0.2 g PVP was added. The mixture was stirred vigorously for 30 min and then sealed in a Teflon-lined stainless steel autoclave (50 mL capacity). The autoclave was heated to and maintained at 180°C for 12–24 h and then was allowed to cool to room temperature. The dark products were subjected to magnetic decantation, followed by repeated washing with distilled water, ethanol, and acetone. The final products were dried in a vacuum oven at 60°C for 8 h.

Phase and composition analyses of the products were performed by X-ray diffraction/photoelectron spectroscopy [XRD/XPS (Philips X Pert Prodiffractometer with Cu Kα ($\lambda = 1.54056$ Å) radiation)/(AXIS ULTRA XPS, Al Kα)]. The size and morphology of the as-synthesized MSs were investigated by using scanning/transmission electron microscopy (SEM/TEM, JSM5600LV/JEOL100CX-II). The magnetic measurements were carried out by a vibrating sample magnetometer (VSM).

Results and Discussion

Figure 1a shows a typical XRD pattern of the as-fabricated sample (reaction for 24 h). All diffraction peaks can be indexed to a simple cubic lattice (FCC), and the positions along with relative intensity of peaks match well with standard $CoFe_2O_4$ powder diffraction database (JCPDS File No. 22-1086), indicating that the as-obtained products have an Fd3m cubic spinel structure. According to the Scherrer equation, the average crystallite size which is calculated based on the XRD pattern (311) is approximately 8 nm. In fact, the XRD patterns of the others (reaction for 12 and 36 h) are similar to it (not shown). More accurately, XPS was used to determine its composition. Figure 1b and c show the high-resolution XPS spectra of 2p Co and Fe, respectively. The peak at 780.8 eV is from $Co2p_{3/2}$, with a shake up satellite at 785.9 eV, while the peak at 797.2 eV is caused by $Co2p_{1/2}$, with a satellite peak at 803.0 eV. The presence of those two peaks and the highly intense satellites near them is consistent with the presence of Co^{2+} in the high-spin state. All the Fe2p spectra generally show a main peak at a binding energy (BE) of around 710.3 eV, accompanied by a satellite line visible at a BE of around 718.3 eV, only indicative of the presence of Fe^{3+} cations.

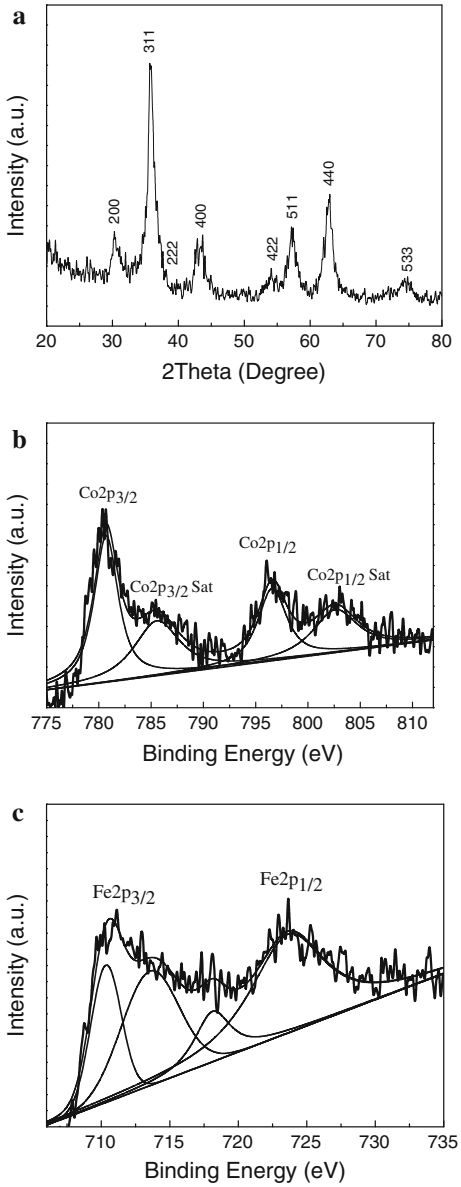

Fig. 1 The as-synthesized $CoFe_2O_4$ MSs for **a** XRD pattern, and XPS spectra **b** Co2p and **c** Fe2p

Further quantitative analysis finds that the atomic ratio between Co and Fe is about 1:2, which is compatible with the data of XRD.

The SEM images of the as-synthesized samples obtained at different reaction times are illustrated in Fig. 2a and b. It is clear that both of the products have uniform spherical shapes. The average size of the $CoFe_2O_4$ MSs is ~220 nm [solvothermal treated for 12 h (Fig. 2a)]. However, when extending the reaction time to 24 h, the average size increases to ~330 nm (as revealed in Fig. 2b). As shown in the corresponding TEM images in Fig. 2c and d, these micrometer-sized $CoFe_2O_4$ spheres [~220 nm (Fig. 2c) and ~330 nm (Fig. 2d) in diameter, respectively] can

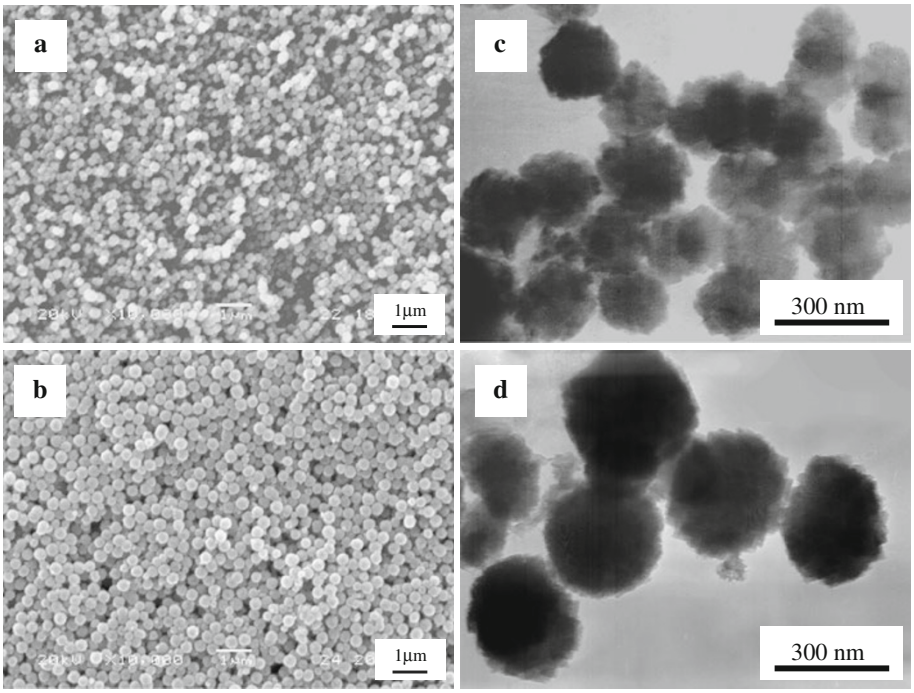

Fig. 2 SEM/TEM images of products prepared at different reaction time: **a/c** 12 h, **b/d** 24 h

clearly be seen. Additionally, an individual sphere is not a single microparticle but the assemblies of small $CoFe_2O_4$ nanoparticles (the diameter of $\sim$8 nm), in which the size of primary nanoparticles is in excellent agreement with the XRD results.

To obtain a better understanding of the formation and evolution of $CoFe_2O_4$ MSs along with the reaction time, that the reaction duration was further extended to 36 h was carried out. The MSs were evacuated resulting in octahedral-shaped $CoFe_2O_4$ particles, which are confirmed by the SEM image (Fig. 3a) and TEM image (Fig. 3b). As a consequence, a proposed mechanism of formation and evolution of the $CoFe_2O_4$ MSs is sketched in Fig. 4. It is well known that PVP can selectively absorb on a certain crystal facet of the as-prepared primary building blocks such as nanoparticles, nanosheets, nanoplates, nanorods, and so on [20–23]. In our experimental system, PVP surfactant contributes not only to preventing these primary building blocks from entropy-driven random aggregation but also to controlling the formation of the regular geometry. The formation and evolution of MSs seems to be as follows: at first, this $CoFe_2O_4$ phase undergoes consequent nucleation and growth around the entire surface stabilized by PVP. In the subsequent process, driven by the minimization of the total energy of the system, the small primary $CoFe_2O_4$ nanoparticles aggregated together to form three-dimensional (3D) spheres. Ostwald ripening occurred under solvothermal conditions, resulting in the formation of $CoFe_2O_4$ spheres from small grows into larger due to isotropic growth. The octahedral shape of the product

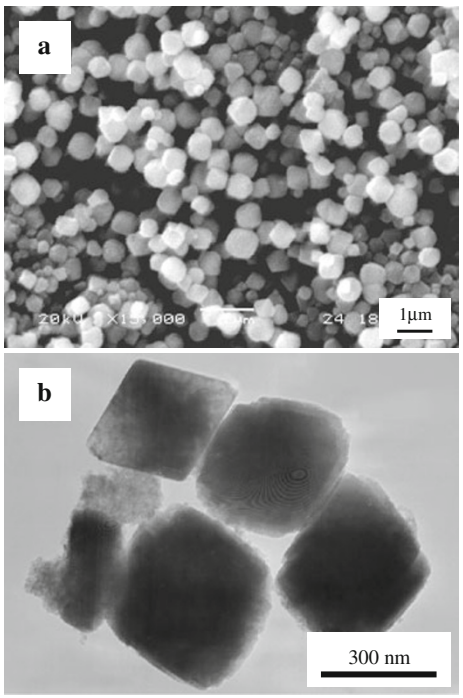

Fig. 3 **a** SEM/**b** TEM images of studied samples with 36 h reaction time

obtained by reaction for 36 h may be explained by combination of thermodynamic aspects of crystal growth and the selective adsorption model of surfactants on different crystallographic facets [24, 25]. Moreover, the structures may be deduced that development of the (111) facets was

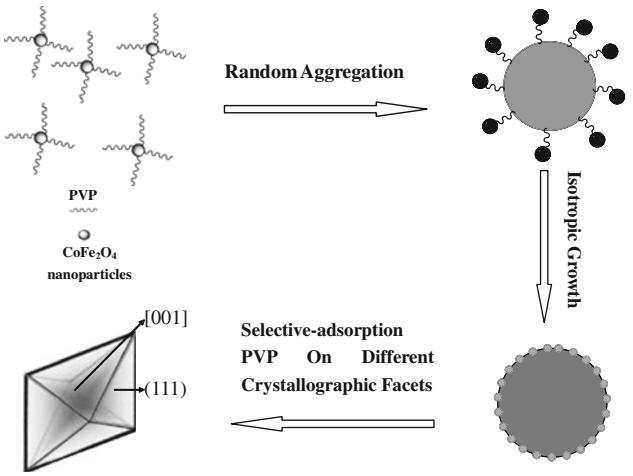

Fig. 4 Schematic illustration of the formation and evolution of $CoFe_2O_4$ MSs along with the reaction time

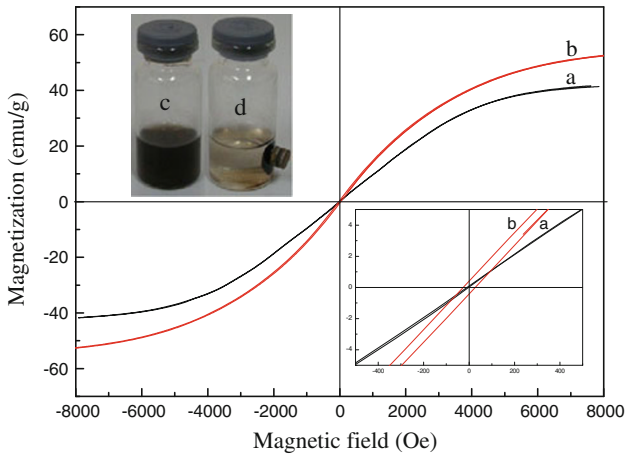

Fig. 5 RT magnetization curves for the of $CoFe_2O_4$ MSs with different reaction time: **a** 12 h, **b** 24 h (The *inset* shows enlarged magnetic hysteresis loops at low applied fields); photographs of $CoFe_2O_4$ MSs dispersion in a vial, **c** without magnetic field, **d** with magnetic field for 1 min

handicapped by the adsorbed PVP surfactant on these facets. Of course, convincing explanation on the mechanism of MSs is our further work.

The magnetic behavior of $CoFe_2O_4$ MSs is very important for practical applications. The room-temperature magnetization curves (Fig. 5a, b) display the two relatively high Ms values of 41.2 (taken from 220 nm) and 55.2 emu/g (330 nm), respectively. Both values are, however, somewhat lower than the bulk value (71.2 emu/g) [18, 19]. The hysteresis loop shows essentially no coercivity (H_C) for the smaller size samples (220 nm) and negligible value of 27 Oe (larger size specimens, a diameter of 330 nm), suggesting that improved coalescence of the crystallites in the nanostructures results in increased magnetic coupling and higher magnetization. According to the results of XRD and TEM observations, the average size of primary crystals is about 8 nm, smaller than the SP critical size of $CoFe_2O_4$ [26, 27]. So it is reasonable that the self-assembled cobalt ferrite MSs reveal SP behavior even though their sphere size exceeds 200 nm. The stabilization of the MSs in distilled water thanks to the surfaces capped of hydrophilic PVP. Slight agitation can bring the MSs to back into the aqueous solution when the magnet is removed (Fig. 5c) although these magnetic MSs can be completely separated from the solution when the solution is subjected to an external magnetic field within minutes, as shown in Fig. 5d. It can be obviously seen that the $CoFe_2O_4$ MSs have rapid magnetic response ability at room temperature, as well as, highly monodispersed, and biocompatible.

Conclusion

In summary, SP $CoFe_2O_4$ MSs have been synthesized through a simple surfactants-assisted solvothermal method at a relatively low temperature. All of the reactants are common reagents and inexpensive, as well as environment benign. The as-prepared MSs, composed of about 8-nm $CoFe_2O_4$ nanoparticles, have uniform sizes (diameters up to several hundred nanometers), high Ms and well water-dispersible make them good candidates for not only in advanced magnetic materials and ferrofluid technology, but also in biomedical fields such as biomolecular separations, targeted drug delivery, as well as magnetic resonance imaging.

Acknowledgments This work was partially supported by the Program for Science & Technology Innovation Talents in Universities of Henan Province (No. 2008 HASTIT002), Innovation Scientists and Technicians Troop Construction Projects of Henan Province (No. 094100510015), and by the Natural Science Foundation of China under Grant No. 20971036.

References

1. A. Skumiel, J. Magn. Magn. Mater. **307**, 85 (2006)
2. S. Neveu, A. Bee, M. Robineau, D. Talbot, J. Colloid Interface Sci. **255**, 293 (2002)
3. H. Shi, Y. Duan, Nanoscale Res. Lett. **4**, 480 (2009)
4. J.H. Lee, Y.M. Huh, Y.W. Jun, J.W. Seo, J.T. Jang, H.T. Song, S. Kim, E.J. Cho, H.G. Yoon, J.S. Suh, Nat. Med. **13**, 95 (2007)
5. M.F. Casula, P. Floris, C. Innocenti, A. Lascialfari, M. Marinone, M. Corti, R.A. Sperling, W.J. Parak, C. Sangregorio, Chem. Mater. **22**, 1739 (2010)
6. S. Cao, Y.J. Zhu, M.Y. Ma, L. Li, L. Zhang, J. Phys. Chem. C **112**, 1851 (2008)

7. J. Xie, S. Peng, N. Brower, N. Pourmand, S.X. Wang, S.H. Sun, Pure Appl. Chem. **78**, 1003 (2006)
8. S. Ghosh, S. GhoshMitra, T. Cai, D.R. Diercks, N.C. Mills, D.L. Hynds, Nanoscale Res. Lett. **5**, 195 (2010)
9. C. Liu, B. Zou, A.J. Rondinone, Z.J. Zhang, J. Am. Chem. Soc. **122**, 6263 (2000)
10. E. Choi, Y. Ahn, S. Kim, D. An, K. Kang, B. Lee, K. Baek, H. Oak, J. Magn. Magn. Mater. **262**, L198 (2003)
11. S. Sun, H. Zeng, D. Robinson, S. Raoux, P. Rice, S. Wang, G. Li, J. Am. Chem. Soc. **126**, 273 (2004)
12. Y. Lee, J. Lee, C. Bae, J. Park, H. Noh, J. Park, T. Hyeon, Adv. Funct. Mater. **15**, 503 (2005)
13. W. Wu, Q.G. He, C.Z. Jiang, Nanoscale Res. Lett. **3**, 397 (2008)
14. R.J. Tackett, A.W. Bhuiya, C.E. Botez, Nanotechnology **20**, 445705 (2009)
15. T. Neuberger, B. Schopf, H. Hofmann, M. Hofmann, B. von Rechenberg, J. Magn. Magn. Mater. **293**, 483 (2005)
16. S.H. Xuan, Y.J. Wang, J.C. Yu, K.C. Leung, Chem. Mater. **21**, 5079 (2008)
17. P. Granitzer, K. Rumpf, A. Roca, M. Morales, P. Poelt, M. Albu, Nanoscale Res. Lett. **5**, 374 (2010)
18. K. Lee, S. Kim, D. Kang, J. Lee, Y. Lee, W. Kim, D. Cho, H. Lim, J. Kim, N. Hur, Chem. Mater. **20**, 6738 (2008)
19. N.Z. Bao, L.M. Shen, Y.A. Wang, J.X. Ma, D. Mazumdar, A. Gupta, J. Am. Chem. Soc. **131**, 12900 (2009)
20. Y. Wei, L. Li, X. Yang, G. Pan, G. Yan, X. Yu, Nanoscale Res. Lett. **5**, 433 (2010)
21. Z.P. Liu, S. Li, Y. Yang, Z.K. Hu, S. Peng, J.B. Liang, Y.T. Qian, New J. Chem. **27**, 1748 (2003)
22. W. Yu, H.Q. Xie, L.F. Chen, Y. Li, C. Zhang, Nanoscale Res. Lett. **4**, 465 (2009)
23. Y.H. Zheng, Y. Cheng, Y.S. Wang, L.H. Zhou, F. Bao, C. Jia, J. Phys. Chem. B **110**, 8284 (2006)
24. H.M. Yang, J. Ouyang, A.D. Tang, J. Phys. Chem. B **111**, 8006 (2007)
25. L.J. Zhao, H.J. Zhang, Y. Xing, S.Y. Song, S.Y. Yu, W.D. Shi, X.M. Guo, J.H. Yang, Y.Q. Lei, F. Cao, Chem. Mater. **20**, 198 (2008)
26. M. Rajendran, R.C. Pullar, A.K. Bhattacharya, D. Das, S.N. Chintalapudi, C.K. Majumdar, J. Magn. Magn. Mater. **232**, 71 (2001)
27. Z.J. Gu, X. Xiang, G.L. Fan, F. Li, J. Phys. Chem. C **112**, 18459 (2008)